Nanoscale

Highly Stable and Re-dispersible Nano Cu Hydrosols with Sensitively Size-dependent Catalytic and Antibacterial Activities

Journal:	*Nanoscale*
Manuscript ID:	NR-ART-05-2015-003414.R1
Article Type:	Paper
Date Submitted by the Author:	29-Jun-2015

Complete List of Authors:	Zhang, Yu; Shenzhen Institutes of Advanced Technology, Chinese Academy of Sciences Zhu, Pengli; Shenzhen Institutes of Advanced Technology, Chinese Academy of Sciences Li, Gang; Shenzhen Institutes of Advanced Technology, Chinese Academy of Sciences Wang, Wenzhao; Shenzhen Institutes of Advanced Technology, Chinese Academy of Sciences Chen, Liang; Shenzhen Institutes of Advanced Technology, Chinese Academy of Sciences Lu, Daniel; Shenzhen Institutes of Advanced Technology, Chinese Academy of Science, Sun, Rong; Shenzhen Institutes of Advanced Technology, Chinese Academy of Sciences Zhou, Feng; Lanzhou Institute of Chemical Physics, Chinese Academy of Sciences Wong, Chingping; Department of Electronics Engineering, The Chinese University of Hong Kong

Journal Name

ARTICLE

Highly Stable and Re-dispersible Nano Cu Hydrosols with Sensitively Size-dependent Catalytic and Antibacterial Activities

Received 00th January 20xx,
Accepted 00th January 20xx

DOI: 10.1039/x0xx00000x

www.rsc.org/

Yu Zhang,‡[a,b,c] Pengli Zhu,‡*[a] Gang Li,[a] Wenzhao Wang,[a] Liang Chen,[a] Daoqiang Daniel Lu,*[a] Rong Sun,*[a] Feng Zhou[b] and Chingping Wong[d,e]

Highly stable monodispersed nano Cu hydrosols were facilely prepared by an aqueous chemical reduction method through selecting copper hydroxide ($Cu(OH)_2$) as the copper precursor, poly(acrylic acid) (PAA) and ethanol amine (EA) as the complexing agents, and hydrazine hydrate as the reducing agent. The size of obtained Cu colloidal nanoparticles was controlled from 0.96 to 26.26 nm by adjusting the dosage of copper precursor. Moreover, the highly stable nano Cu hydrosols could be easily concentrated and re-dispersed in water meanwhile maintaining good dispersibility. A model catalytic reaction of reducing *p*-nitrophenol with $NaBH_4$ in the presence of nano Cu hydrosols with different sizes was performed to set up the relationship between the apparent kinetic rate constant (k_{app}) and the particle size of Cu catalysts. The experimental results indicate that the corresponding k_{app} showed an obvious size-dependency. Calculations revealed that k_{app} was directly proportional to the surface area of Cu catalyst nanoparticles, and also proportional to the reciprocal of particle size based on the same mass of Cu catalysts. This relationship might be a universal principle for predicting and assessing the catalytic efficiency of Cu nanoparticles. The activation energy (E_a) of this catalytic reaction when using 0.96 nm Cu hydrosol as catalyst was calculated to be 9.37 kJ mol^{-1}, which is considered an extremely low potential barrier. In addition, the synthesized nano Cu hydrosols showed size-dependent antibacterial activities against *Pseudomonas aeruginosa* (*P. aeruginosa*) and the minimal inhibitory concentration of the optimal sample was lower than 5.82 $\mu g\ L^{-1}$.

Introduction

Researches on metal colloidal particles have received wide attentions during recent decades because of their size-dependent optical, magnetic, electronic, chemical and other special properties.[1-7] Within these materials, nano copper has always been a hot issue specifically due to its low processing costs and the potential applications in lubrication, electrical and thermal conductivity, nanofluids, and catalytic reactions.[8-12] While the basic properties of Cu colloidal particles mainly depend on their size, shape, crystallinity and structure, which exactly determine their practical applications. Therefore, the preparation of monodispersed nano Cu colloids with controllable size and shape continues to be of considerable interest.

Among the numerous synthesis methods of metal colloids, wet-chemical approach appears to be the most promising strategy for industrial applications by virtue of its intrinsic superiorities: the striking synthetic simplicity, the avoidance of complex and demanding apparatus, the easy control of size and shape.[13-15] The key parameters that affect the size and shape of nanoparticles in wet-chemical synthesis include the ratio of stabilizers to the precursor salts, chemical nature of the stabilizers and the control of reaction kinetics through rapid nucleation and growth.[16-19] However, compared with other noble metals, such as Ag and Au, the synthesis of stable, monodispersed and uniform nano Cu colloidal particles in such a way has been proven to be difficult because of its extreme sensitivity to oxygen and colloidal agglomeration. Hence, in order to minimize the oxidation and agglomeration of copper nanoparticles, extreme experimental conditions, such as using non-aqueous solvent, low concentration of precursors with various stabilizers and also under the protection of inert gas, are needed. In previous reports, *Mott et.al* described an investigation of preparing Cu nanoparticles with controlled sizes and potentially shapes by a combination of controlled reaction temperature and capping agents in organic solvents under argon gas.[10] *Yu* and his co-workers successfully synthesized spherical Cu nanoparticles with controllable size by a modified reverse micelle method with oleic acid and oleylamine as surfactants in mixed solvents of water and xylene.[20] Although there are plenty of approaches to synthesize nano Cu colloidal particles under specific conditions

[a] *Shenzhen Institutes of Advanced Technology, Chinese Academy of Sciences, Shenzhen, China.*
[b] *State Key Laboratory of Solid Lubrication, Lanzhou Institute of Chemical Physics, Chinese Academy of Sciences, Lanzhou, China.*
[c] *Shenzhen College of Advanced Technology, University of Chinese Academy of Sciences, Shenzhen, China.*
[d] *School of Materials Science and Engineering, Georgia Institute of Technology, Atlanta, USA.*
[e] *Department of Electronics Engineering, The Chinese University of Hong Kong, Hong Kong, China.*
† Electronic Supplementary Information (ESI) available. See DOI: 10.1039/x0xx00000x
‡These authors have equally contributed to the work.

in non-aqueous solvent, relatively limited attempts have been succeeded in synthesizing nano Cu hydrosols with controllable size and shapes. This is mainly because, compared with nano Cu colloids synthesizing in organic solvent, the nano Cu hydrosols may suffer from more serious stability problems in practice. The much more dissolved oxygen in water would reduce the chemical stability of copper nanoparticles and the low viscosity of aqueous solution also makes it harder to keep copper nanoparticles physically stable. Hence, maintaining long-term stability is a vital factor for determining the performance of nano Cu hydrosols. To date, few methods have been established to synthesize the monodispersed nano Cu hydrosol effectively with controllable size, shape, as well as long-term stability in aqueous solvent without the protection of inert gas. Therefore, to synthesize nano Cu hydrosols with controllable size, shape and high stability at mild conditions, a simple chemical reduction strategy is highly desired.

Herein, we report a facile chemical reduction method to synthesize monodispersed and spherical Cu colloidal nanoparticles of controllable size in aqueous solution without protective gas. The size of nano Cu hydrosols was easily changed through adjusting the dosage of copper precursor (namely the ratio of copper precursor and protective agents). Meanwhile, the long-term stability and re-dispersibility of nano Cu hydrosols were confirmed experimentally. These highly stable nano Cu hydrosols with various sizes were employed as catalysts in an organic reaction to demonstrate their potential for catalysis. The influences of particle size on the apparent kinetic rate constant of the catalytic reaction were investigated and the activation energy with the Cu hydrosol catalyst possessing the highest catalytic activity was calculated. In addition, size-dependent antibacterial activities of the synthesized nano Cu hydrosols were clearly observed and most of these nano Cu hydrosols significantly inhibited the growth of a drug-resistant pathogen *P. aeruginosa*.

Experimental

Materials

$Cu(OH)_2$ was purchased from Aladdin Reagent Co., Ltd. Polyacrylic acid (PAA) aqueous solution (mass fraction of 50%), ethanol amine (EA), hydrazine hydrate (mass fraction of 85%), p-nitrophenol (4-NP, $C_6H_5NO_3$), sodium borohydride were purchased from Sinopharm Chemical Reagent Co. Ltd. (China). Deionized water was used in all experiments.

Preparation of the nano Cu hydrosols

In a representative preparation process, PAA and EA were sequentially added into the $Cu(OH)_2$ aqueous solution, presenting a few bubbles with the color changing from sky-blue to dark-blue. The reduction was initiated by the addition of hydrazine hydrate and accompanied with the color of system gradually turning to reddish brown. The whole reaction process was conducted at room temperature and the reddish aqueous phase in equilibrium indicated the reduction of Cu^{2+} to Cu^0 NPs. The yielded Cu hydrosols were manifested various size by varying the dosages of copper precursor. The samples were numbered from S1 to S6 in turn according to the different copper source usage (0.001mol, 0.005mol, 0.010mol, 0.015mol, 0.020 mol, and 0.025 mol).

Characterization

Characterizations of the samples were carried out by different techniques. The morphology and size of the synthesized Cu hydrosols were observed with transmission electron microscope (TEM, FEI Tecnai G2F20S-TWIN). And the size distributions of Cu colloidal particles were determined through laser particle analyzer (Malvern Zetasizer Nano ZS90, England). The powder X-ray diffraction (XRD) patterns were recorded on an X-ray diffractometer (Rigaku D/Max 2500, Japan) with monochromated Cu-Kα radiation (λ = 1.54 Å). Ultraviolet-visible spectroscopy (UV-Vis) absorption spectra of the samples were recorded on an UV-Vis-NIR spectrometer (Shimadzu UV-3600, Japan) with a wavelength range of 250-800 nm. All measurements were performed at the room temperature.

Evaluation of the size-dependent catalytic activities

Typical organic 4-NP was selected as the catalytic reduction target analyte to evaluate the catalytic performances of the prepared Cu hydrosols in the presence of $NaBH_4$. Also, the reduction of 4-NP without Cu catalyst was carried out as the control experiment.

In a typical activity test process, 100 μl S1 solution was added to 30 mL 4-NP aqueous solution (0.2 mM) followed by addition of 10 mL freshly prepared $NaBH_4$ solution (25 mM). Time-dependent absorption spectra and corresponding kinetic curves during the catalytic reduction of 4-NP were recorded on a UV-Vis-NIR spectrophotometer by placing 2.5 mL of sample solution into a 3 mL quartz cell. Catalytic reduction effects of Cu hydrosols with different particle sizes were detected under the precondition of same copper content. Hence we fixed the mass of Cu nanoparticles used in each catalytic reduction process to well investigate the influence of particle size on the catalytic effect. And the details is shown in Table S1.

Evaluation of the size-dependent antibacterial properties

Synthesized Cu hydrosols with different sizes were investigated for their antimicrobial activity. A clinical isolated *P. aeruginosa* was used as the test bacterium. Bacteria were grown overnight in Luria-Bertani (LB) broth with shaking (220 rpm) at 37 °C. The overnight culture of *P. aeruginosa* was diluted to OD_{600} 0.02 in freshly autoclaved LB medium with 1.5% agar before solidification, and then the mixed culture was poured into plates. To study the antibacterial effects, 5 μL of Cu hydrosols with different sizes under the same concentration were dropped on the plates. Also, the blank sample, S0, without copper particles but containing the rest reaction organics was taken as control. The inhibition halo was measured after 24 h incubation at 37 °C.

To get the minimal inhibitory concentrations (MIC) against *P. aeruginosa*, the Cu hydrosols that has the best bacteriostatic effect mentioned above was diluted into 25 mL fresh LB broth to a range of concentrations. Overnight bacteria culture was inoculated to LB medium with or without Cu hydrosols to a final OD_{600} of 0.005. LB medium and LB with corresponding

concentration of S0 were used as control. Flasks were incubated at 37 °C and 220 rpm and culture tubidity (OD_{600}) were measured periodically during the cultivation period. All experiments were performed in duplicate under sterile conditions.

Results and discussion

Fig. 1 (left panels) shows typical TEM images of the as-synthesized Cu nanoparticles using different dosages of copper precursor (S1 to S6 corresponding to 0.001 mol, 0.005 mol, 0.010 mol, 0.015 mol, 0.020 mol and 0.025 mol of copper precursor, respectively). Overall, the particles are isotropic and spherical. Specifically, with the minimum copper source used (Fig. 1-S1), the mean particle diameter of the obtained copper nanoparticle is less than 1 nm. The HRTEM images of S1 (Fig. S1) also illustrate the nanoparticles to be Cu crystals, in which the measured lattice d-spacing (0.2096 nm, 0.2105 nm and 0.2105 nm) are consistent with interplane distance value of (111) in face-centered cubic Cu crystal. Then the size of synthesized nano Cu hydrosols gradually grows larger with the increased dosages of copper source (Fig. 1-S1~S5). When the dosage approached to 0.025 mol (Fig. 1-S6), the resulting particle size was about 26.26 nm. Fig. S2 (the XRD pattern of S6 after centrifugal washing) demonstrates again that phase-pure Cu with face-centered cubic crystal structure were obtained. The histograms of corresponding Cu colloidal nanoparticle size distributions are presented in Fig. 1 (right panels). Results indicate that the sizes of the Cu colloidal nanoparticles with various dosages of copper precursor are 0.96 nm, 2.01 nm, 5.21 nm, 9.42 nm, 17.36 nm and 26.26 nm, respectively. All samples present high monodispersity and narrow particle size distributions. These results are well consistent with the TEM observation. Fig. 2a reveals the relationship between the dosages of copper precursor and the size of generated Cu colloidal nanoparticles. It indicates that the average size of the prepared nano Cu hydrosols monotonically grows with increasing the dosages of copper precursor or the molar ratio of Cu^{2+}/PAA-EA in the reaction. Therefore, monodispersed and spherical nano Cu hydrosols with controllable size could be easily achieved by adjusting the dosages of copper source in aqueous solution without protective gas.

UV-Vis spectroscopy was also performed to monitor the size variation of the synthesized nano Cu hydrosols. It is known that metal nanoparticles exhibit absorption bands in the UV-Vis range due to their metallic nature (the excitation of surface plasmon resonance), and their surface plasmon resonance (SPR) greatly depends on the size, morphology, surface state and the surrounding medium environment of the colloidal particles.[21] In general, the SPR peaks may slightly red-shift and the band broadens as the metal particle size increasing.[22] Fig. 2b shows the UV-Vis absorption spectra of synthesized nano Cu hydrosols with different dosages of copper source. It is clearly observed that red shift and gradual broadening of the SPR peaks with the increase of particle size, which is consistent with the general trend. Specifically, the surface plasmon peaks of the synthesized nano Cu hydrosols in S1 and S2 both appear at around 560 nm, which are consistent with the known value.[22, 23] With the gradually increased dosage of copper source, the surface plasmon peaks of the colloidal nanoparticles showed red-shift and also exhibited relatively

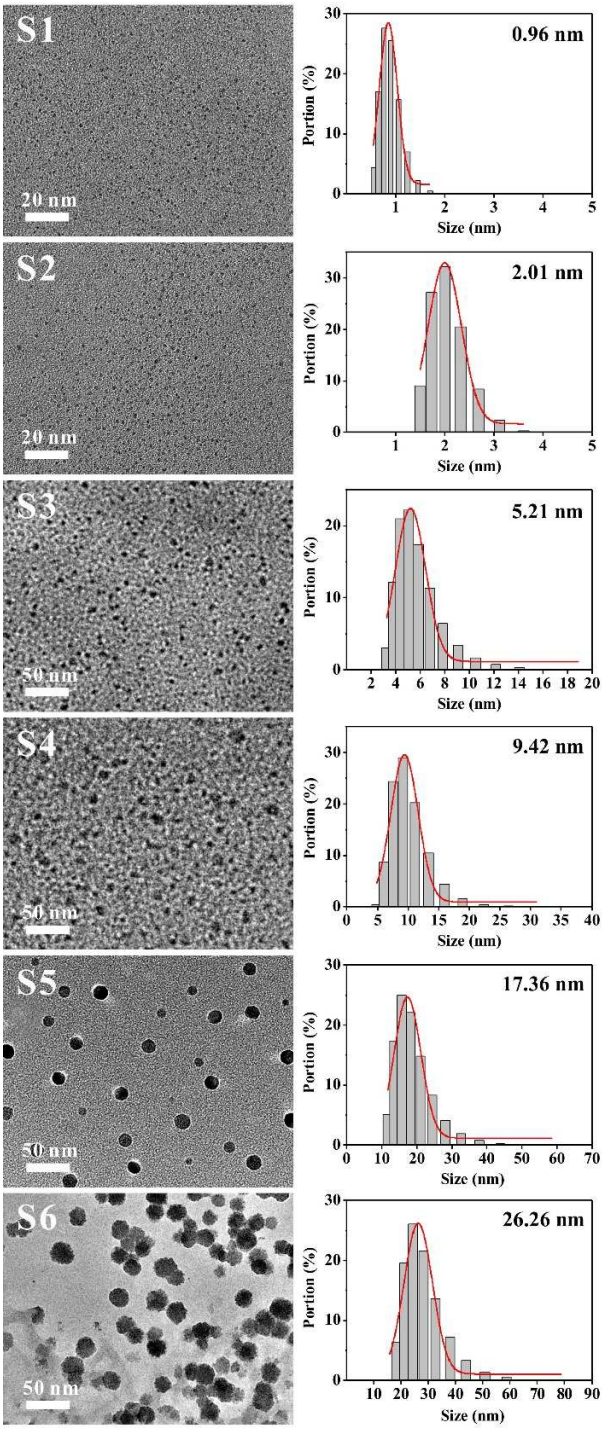

Fig. 1 TEM images and size distributions of synthesized nano Cu hydrosols with different dosages of copper source.

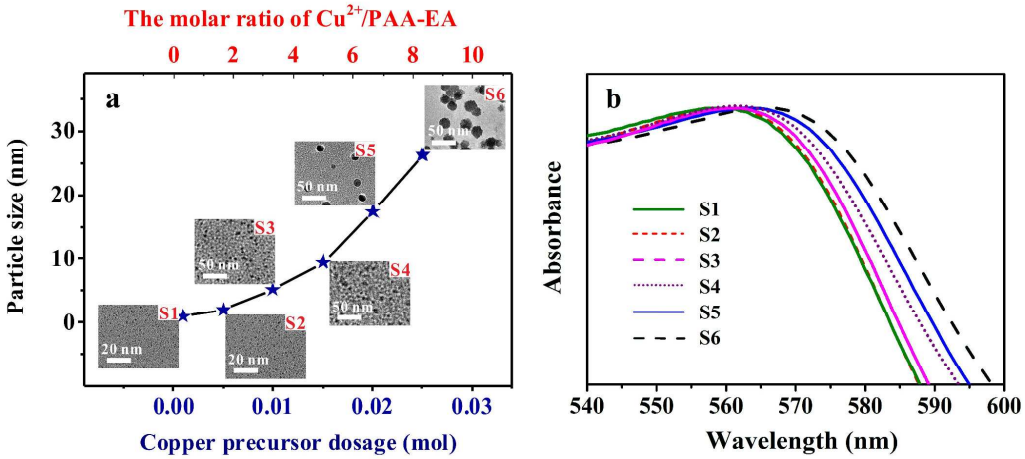

Fig. 2 a) Size dependence of the synthesized nano Cu hydrosols on the dosages of copper source, from left to right are in the order of S1~S6, respectively; b) UV-Vis absorption spectra of the formed Cu hydrosols with different particle size.

broadened distributions. This also indirectly indicated that obtained Cu hydrosols became larger in size along with the increased dosage of copper source.

Cu nanoparticles tend to be fairly unstable in aqueous solution and therefore, special precautions have to be taken to avoid their aggregation or precipitation in the later placement. Fig. 3a shows the images of the nano Cu hydrosol (S1) when it was prepared and after stored at room temperature for 400 days. It is seen that the hydrosol after long-term storage also exhibited good dispersity without obvious aggregation or precipitation just as the freshly prepared. Simultaneously, another operation was carried out to evaluate the stability through concentrating and re-dispersing the original nano Cu hydrosol. After concentrating by using rotary evaporation at 80 ^{o}C, the excessive water, EA and hydrazine hydrate in the mixture could be largely removed, while PAA-EA chains remained in the solution due to its high boiling point. After concentrating from 100 mL down to 3 mL, the solution still maintained high dispersibility without aggregation or precipitation (Fig. 3b). Subsequently, the concentrated nano Cu hydrosol was re-dispersed into 100 mL aqueous solution via shaking and mixing, and the good dispersibility was observed. Besides S1, all other samples (S2~S6) show similarly good stabilities and re-dispersibilities, in which pictures of S6 are shown in Fig. S3. This easily concentrated and re-dispersed performance will be good for the storage and applications of the nano Cu hydrosols. The reason might be attributed to the space steric hindrance of PAA-EA chains that prevents the aggregation or precipitation of copper nanoparticles. More detailed discussion will follow in later section of this paper.

Fig. 3 a) The nano Cu hydrosol of freshly prepared and after placing for 400 days; b) The original nano Cu hydrosol after concentration and re-dispersion.

In order to improve understanding of the growth process and stability of nano Cu hydrosols, the possible reaction mechanism is illustrated in Fig. 4. First, a small amount of Cu^{2+} ions could be released by dissolving copper hydroxide into the aqueous solution. After addition of PAA, Cu^{2+} ions are chelated with the carboxyl groups along the PAA chains to form PAA-Cu^{2+} complex. This weak acid environment and complexation reaction would render more and more dissolution of $Cu(OH)_2$ and subsequent formation of PAA-Cu^{2+} complex. Then, the introduction of EA not only forms polymer chains with PAA, in which the exposed N would be chelated with Cu^{2+} to form a more stable structure, but also provides an alkaline environment for the subsequent reduction reaction. In this process, if the dosage of the copper precursor is low, *e.g.* 0.001 mol in S1, the ionized Cu^{2+} could be completely chelated with PAA-EA chains since PAA-EA chains are in excess. As we fixed the amount of PAA and EA molecules in the mixture, the number of Cu^{2+} ions bonded with each PAA-EA chain gradually increase as the amount of copper precursor increases. Subsequently, the Cu^{2+}-PAA-EA complex is reduced by hydrazine hydrate and the Cu^{2+} bonded in the PAA-EA chains are in situ transformed to Cu nanoparticles. The number of PAA-EA polymer chains coated on the surface of each Cu^{2+} ion influences the nucleation, growth process, and final particle size of Cu nanoparticles. TG tests of several samples were also

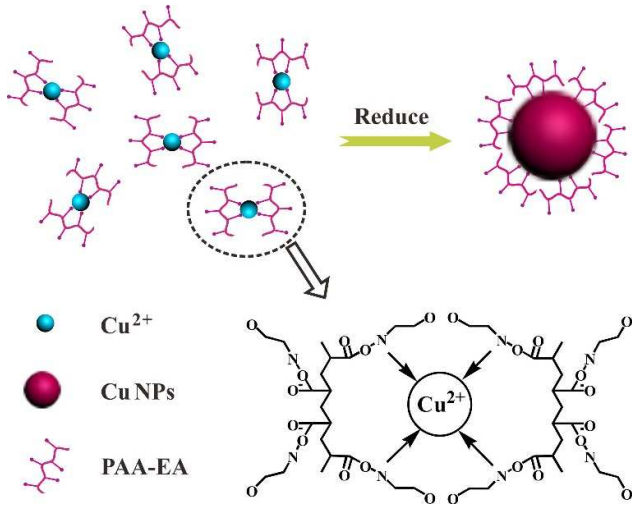

Fig. 4 Scheme of the synthetic mechanism of nano Cu hydrosols.

carried out to determine the amount of polymer chains on the surface of nanoparticles (Fig. S4). Results indicate that from S3 to S6, the particle size increases, following with organics coating on the surface of single particle decreasing gradually. It is precisely because the different amount of polymer chains on the surface of each particle that resulting in the different size of copper nanoparticles. Meanwhile, the water-soluble carboxylate groups of PAA-EA could completely encapsulate the generated Cu colloidal nanoparticles to prevent them from aggregation and precipitation, and provides nano Cu hydrosols with excellent stability and re-dispersibility due to the large steric hindrance of the coated organic chains. In addition, it should be noted that, compared with other copper salts like copper nitrate, copper chloride and *etc.*, the copper hydroxide does not introduce any impurity ions which would be detrimental to practical applications.

Catalytic activity of metal particles is mostly studied using model reactions, which can effectively monitor the reaction kinetics. In this study, the model reaction of catalytic reduction of 4-nitrophenol (4-NP) to 4-aminophenol (4-AP) with $NaBH_4$ was performed because the maximum absorption of the organic does not overlap with that of the surface plasmon resonance of Cu colloidal nanoparticles. When the reduction was started, the absorbance at 400 nm for 4-nitrophenolate anion gradually decreases accompanied with a new absorption peak at 300 nm, indicating the formation of 4-AP.[24-26] Therefore, this reduction procedure can be feasibly monitored by time-dependent UV-Vis absorption spectra. Furthermore, the catalytic effect of metal particles in principle greatly depends on the specific surface area which is directly related to the particle size.[27-29] Here we fixed the mass of Cu nanoparticles used in each experiment so as to well investigate the influence of particle size on the catalytic effect. Fig. 5 shows the time-dependent UV-Vis absorption spectra in the presence of as-synthesized catalysts (S1-S6). In the presence of S1, the absorption peak of 4-NP at 400 nm decreased rapidly with time and a new peak at 300 nm concomitantly appeared. The disappearance of the 400 nm-peak marked the complete conversion from 4-NP to 4-AP, which took 6 min. For S2 and S6, the whole catalytic reduction process lasted for 18 min and 100 min, respectively. The entire trend showed an apparent size-dependent behavior. For the control experiment, catalytic reductions of 4-NP by NaBH4 without hydrosol (Fig. S5a) and with S0 which only contains hydrosol organics without copper nanoparticles (Fig. S5b) were also carried out. The absorption peak both showed no apparent change with time, confirming that 4-NP could only be reduced in the presence of Cu nanoparticles. This phenomenon can be explained as follows:

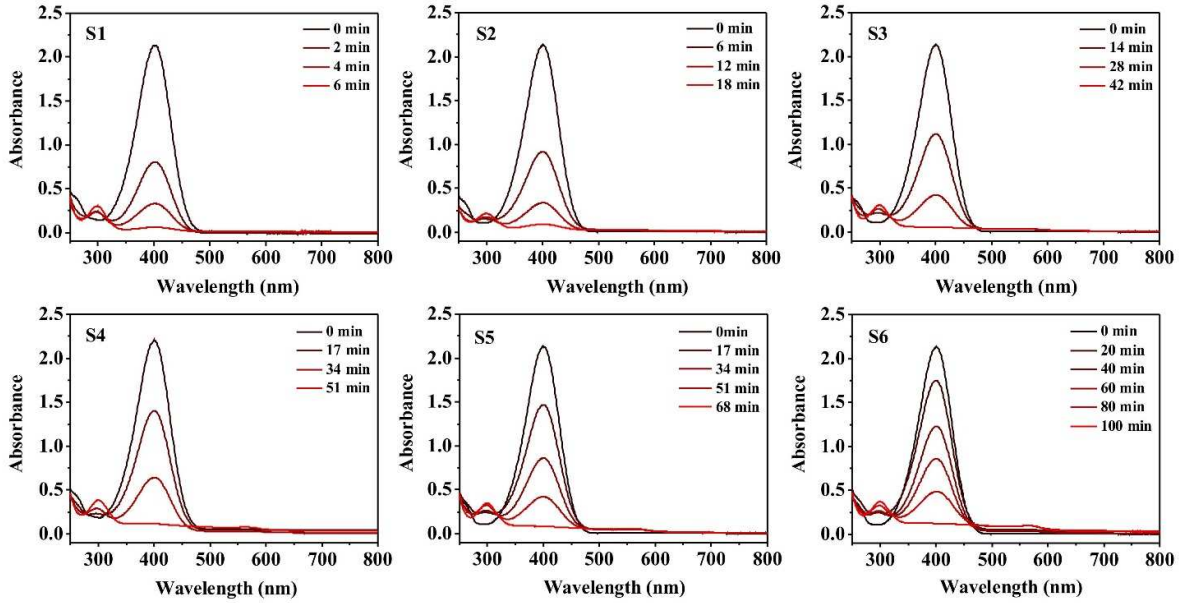

Fig 5. UV-Vis absorption spectra of catalytic reduction of 4-NP by $NaBH_4$ with synthesized nano Cu hydrosols S1-S6, respectively.

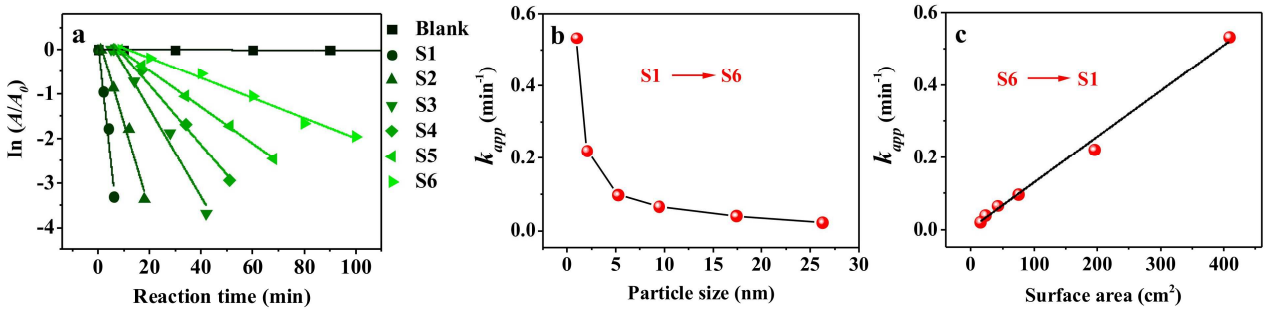

Fig. 6 a) Plots of ln(A/A_0) against the reaction time *t*; b) and c) The relationship between k_{app} and the particle size, the resulting surface area, respectively.

although the reduction of 4-NP into 4-AP is a thermodynamically favorable process in which E_0 for 4-NP/4-AP = -0.76 V and H_3BO_3/BH_4^- = -1.33 V versus NHE, from the kinetic point of view, it is unfavorable. In other words, nano Cu hydrosol plays a critical role in catalyzing reduction process and the corresponding catalytic efficiency can be dramatically improved as the particle size gradually decreases.

Kinetically, this catalytic reaction could be regarded as pseudo-first-order reaction relative to 4-NP considering the amount of reductant $NaBH_4$ is excessive.[26] In order to get the apparent kinetic rate constant k_{app} (min^{-1}) of the different Cu catalysts, the reaction kinetics was calculated separately by real-time monitoring their time-dependent UV-Vis absorption spectra. Here, ln(A/A_0) versus the reaction time *t* (min) for the catalytic process was plotted in Fig. 6a. It exhibits good linear relationship under different catalysts, confirming that the catalytic reduction of 4-NP follows the pseudo-first-order kinetics. The rate constants can be easily obtained from the slope of the kinetic curves (Table S1) while fixing other variables including the initial 4-NP concentration, borohydride concentration, and copper content in the catalysts. It can be seen from Fig. 6 that the value of k_{app} for the reduction without catalyst is very low, and the addition of nano Cu hydrosol greatly accelerates the reducing reaction. Also, catalytic efficiency of the nano Cu hydrosol increases with decreased particle size.

Since electron transfer of catalytic reaction between the organic 4-NP and reducing agent $NaBH_4$ takes place on the surfaces, the nano Cu hydrosols with large surface areas could act as good substrates for the electron transfer and accelerate the reaction. Fig. 6b and c plot the correlation between apparent kinetic rate constants k_{app} with Cu hydrosol particle size and surface area, respectively. The effect on particle size to k_{app} is non-linear. k_{app} decreases sharply initially with particle size increase, and then levels off after S3. From Fig. 6c, it can be seen that k_{app} exhibits linear correlation with the surface area of nano Cu hydrosols. The extrapolation based on this linear relationship is helpful to predict the possible k_{app} value when using Cu nanoparticles with a certain surface area or particle size for our reaction system. According to the fitting results of Fig. 6c, the relation between apparent kinetic rate constant k_{app} and surface area could be described as

$$k_{app} = 0.0012 S_{total} \qquad (R^2 > 0.9919)$$

where S_{total} (the total surface area of catalyst in the reaction system) is equal to the product of S_{single} (the surface area of a single catalyst particle) and *N* (the number of catalyst particles). Therefore, the equation can be further expressed as

$$\begin{aligned} k_{app} &= 0.0012 S_{single}\, N \\ &= 0.0012 \times 4\pi \left(\frac{D}{2}\right)^2 \frac{m_{used}}{m_{single}} \\ &= 0.0012 \times 4\pi \left(\frac{D}{2}\right)^2 \frac{nM\dfrac{V_{used}}{V_{total}}}{\rho V_{single}} \\ &= 0.0012 \times 4\pi \left(\frac{D}{2}\right)^2 \frac{nMV_{used}}{\rho \dfrac{4}{3}\pi \left(\dfrac{D}{2}\right)^3 V_{total}} \\ &= \frac{0.0036}{\rho} \times \frac{nMV_{used}}{\left(\dfrac{D}{2}\right) V_{total}} \\ &= \frac{0.0072}{\rho} \times \frac{m_{used}}{D} \end{aligned}$$

where *D*, m_{used} and m_{single} are the diameter of copper catalyst nanoparticles (particle size), the total mass of copper nanoparticles used, and the mass of a single copper nanoparticle, respectively; *n*, *M* and ρ are the molar of used catalyst, the molar mass and the density of Cu, respectively; V_{used}, V_{single}, and V_{single} are the volume of catalyst used, the volume of total hydrosol, and the volume of a single copper nanoparticle, respectively. This simplification enables facile evaluation of the relationship between apparent kinetic rate constant k_{app} with the size and concentration of catalyst. From the equation above, k_{app} is directly proportional to the m_{used}/D where m_{used} is fixed through controlling the volumes of nano Cu hydrosols and *D* is dependent on the copper source. In other words, under the fixed copper content, k_{app} presents an approximate linear relationship with the reciprocal of copper nanoparticle size in our hydrosol system. In order to confirm our inferences, the real relationship between k_{app} and the reciprocal of the particle size has

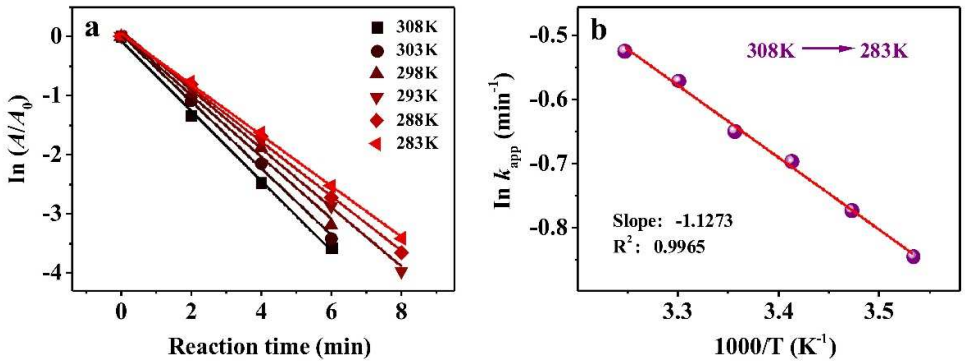

Fig. 7. a) Plots of ln(A/A_0) against the reaction time t; b) Plot of lnk_{app} against 1000/T.

been shown in Fig. S6. Obviously, they have a good linear correlation with each other, which is exactly consistent with the previous deduction.

Activation energy (E_a) is an empirical parameter in chemical reactions, which shows the temperature dependence upon the rate constant for a catalysis reaction. The Arrhenius formula shows

$$\ln k_{app} = \ln A - \frac{E_a}{RT}$$

where A is a constant known as the Arrhenius factor, kapp is the apparent rate constant of the reaction at temperature T (in Kelvin), and R is the universal gas constant.[25] The values of activation energy were calculated from the plot of lnk_{app} against 1/T. Therefore, in order to calculate E_a of the catalytic reaction with catalyst S1 that possesses the most excellent catalytic property, catalytic reduction of 4-NP under different temperatures (308 K, 303 K, 298 K, 293 K, 288 K, and 283 K) were performed to obtain the k_{app} values. From the time-dependent UV-Vis absorption spectra (Fig. S7), we can conclude that with lowering the reaction temperature, the required time for the entire reaction gradually became longer. Fig. 7a presents the relationship between ln(A/A_0) and the reaction time t under different temperatures. According to the linear slopes, the obtained corresponding k_{app} are listed in Table S2. The fitting results show that with the decrease of the reaction temperature, the value of k_{app} is also gradually reduced. Next, we plotted the resulting lnk_{app} against 1000 T^{-1} in Fig. 7b. The plot shows a straight line with a slope of (-E_a/R). Therefore, E_a of the catalytic reaction with S1 could be calculated to be 9.37 kJ·mol^{-1} through the linear fitting. According to the literatures[24, 25, 30-33], the value of E_a for metal-nanostructure catalyzed conversion of 4-NP to 4-AP is generally more than 20 kJ mol^{-1} (Table 1 and Table S3). Compared with other noble metals such as Pd, Pt and Au which generally have high catalytic activities, the obtained E_a of the synthesized Cu nanoparticles is surprisingly the lowest. This is probably because the catalytic reductions occur via surface catalysis mechanism. Therefore, the potential barrier for metal-nanostructure catalyzed reactions largely depends on the size and shape of nanoparticles.

Table 1 Comparison of activation energy E_a for catalytic reduction of 4-NP with $NaBH_4$ in our work and the relevant literatures.

Ref.	Catalyst type	E_a (kJ mol^{-1})
Our work	Cu hydrosol	9.37
Gupta[30]	Fe@Au ATPGO	9.75
Zhang[31]	Cu cubes	22.44
Yamamoto[30]	Au nanoclusters	31
Kalekar[32]	Pt nanoballs	6.4
	Pt nanonets	26
Zeng[25]	Au-Based nanocages	28.04±1.43
	Au-Based nanoboxes	44.25±2.62
	Au-Based partially hollow nanoboxes	55.44±3.15
Mahmoud[24]	Pt-Pd alloy nanocages	109.67±7.53
	Pd nanocages	94.60±6.28
	Pt/Pd nanocages	77.44±5.44
	Pd/Pt nanocages	86.65±7.53
	Pt nanocages	67.81±4.60

P. aeruginosa is an aerobic Gram-negative coccobacillus which would cause widely severe disease in animals, plants and humans.[34] It is one of the most concerned opportunistic pathogen and commonly used for the antimicrobial material research due to its drug-resistant properties and ability to rapidly develop resistance to multiple classes of antibiotics. The growth inhibitory effects of the prepared nano Cu hydrosols against *P. aeruginosa* were evaluated. Firstly, Cu hydrosols with different sizes were diluted to the same concentration (0.0091 M). The formation of inhibition zones

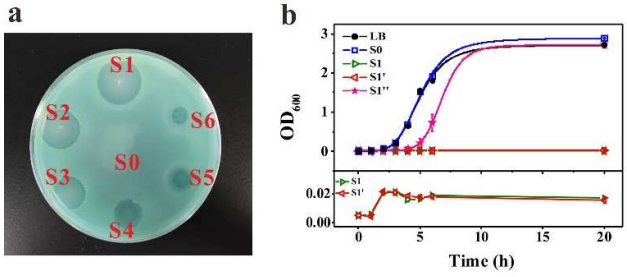

Fig. 8 a) The inhibition zones of S0~S6 against *P. aeruginosa*; b) The growth curves of *P. aeruginosa* under different conditions.

Table 2 Comparison of MIC against *P. aeruginosa* in our work and the relevant literatures.

Ref.	Antibacterial type	Bacteria	MIC
Our work	Cu hydrosol	*P. aeruginosa*	5.82 μg L^{-1}
Mohan[35]	Ag NPs		6 μg mL^{-1}
Prucek[36]	Ag NPs		1.7 mg L^{-1}
	Ag@Fe_3O_4/Ag		15.6/0.9 mg L^{-1}
	γ-Fe_2O_3@Ag/Ag		31.3/3.3 mg L^{-1}
Li[37]	Cu/PAA composites		0.59 μg mL^{-1}
Lokina[38]	Ag NPS		0.3125 mg ml^{-1}

indicates the antimicrobial activity of the tested materials. Fig. 8a reveals the significant inhibition of bacterial growth for S1~S6. The sample S0 which only contains hydrosol organics without copper nanoparticles did not show any inhibition effect, suggesting a lack of antimicrobial activity, which could also rule out the influence of organics in the hydrosol. It was observed that the antibacterial effect strengthened (*e.g.* the inhibition zone got bigger) with decreased particle size. The size-dependent antibacterial activity of nanoparticles is in agreement with other reports.[39, 40] The smaller particles possessing a larger surface area provide a more efficient means in antibacterial activity than larger particles.

Growth studies with optical density (OD) using UV-Vis spectrophotometer were used to evaluate the antimicrobial activity in a quantitative manner. First, sample S1 possessing the best antibacterial effect were diluted to the concentration of ten percent and one hundred percent (recorded as S1' and S1'' respectively) to examine the growth of *P. aeruginosa*. The freshly grown axenic culture of *P. aeruginosa* was inoculated into flasks containing LB medium and various concentrations of nano Cu hydrosols (S1, S1', and S1''). The total volume of liquid medium in each flask was kept at 25 mL and the final concentrations of copper nanoparticles in the liquid medium were 58.2 μg L^{-1}, 5.82 μg L^{-1}, and 0.582 μg L^{-1}, respectively. The growth curves of *P. aeruginosa* under the diverse environment were depicted in Fig. 8b. Without Cu hydrosol supported (LB), the bacteria multiplied in a logarithmic manner from the third hour. The nearly identical growth curve with S0 in LB indicates again that the organics in nano Cu hydrosol had no antibacterial activity. After adding S1 and S1', the growth of bacteria was distinctly suppressed and the logarithmic growth disappeared. There was no longer proliferation after the third hour. However, for S1'', the concentration of which was 100 times diluted, the logarithmic growth was postponed to the fifth hour. The above results demonstrate that the minimal inhibitory concentration (MIC) of S1 (Cu hydrosol with a particle size of 0.96 nm) is below 5.82 μg L^{-1}, which is far below the reported (Table 2).[35-38] The prepared nano Cu hydrosols possessing such excellent antibacterial activities are probably due to the ultra-high specific surface area and uniform dispersion of copper nanoparticles.

Conclusions

By varying the dosages of the copper source, size-controllable nano Cu hydrosols from 0.96 nm to 26.26 nm were obtained in the presence of stabilizing agents of PAA and EA without any additional pH stabilization, inert atmosphere, or organic solvents. Essentially, tuning the molar ratio of copper source to stabilizing agents is found very effective in the size-controllably preparation of monodispersed nano Cu hydrosols. The highly stable and water-dispersible Cu colloid not only could endure long-time room temperature storage without any agglomeration and precipitation, but also could maintain good-dispersibility even after concentration and re-dispersion. Furthermore, the synthesized nano Cu hydrosols exhibit excellent catalytic activities in the reduction of 4-NP in which the apparent rate constant k_{app} significantly increased with the particle size decreasing. The results reveal that the corresponding k_{app} is directly proportional to the surface area of the particle, and also proportional to the reciprocal of particle size based on the same copper content. This relationship probably could be applied to estimate the catalytic activity of other particle size in this hydrosol system. The activation energy of the reaction using the minimal size Cu hydrosol as the catalyst could be as low as 9.37 kJ mol^{-1} due to its high specific surface area. In addition, the nano Cu hydrosols displayed a size-dependent antibacterial activities against *P. aeruginosa* and the MIC of which is lower than 5.82 μg L^{-1}. We believe that these size-controllable nano Cu hydrosols possess a broad application prospect that would be applied to the conductive pastes and other aspects.

Acknowledgements

This work was financially supported by the National Basic Research Program of China (973 Program) (2012CB933700-G), Guangdong Innovative Research Team Program (No. 2011D052 and KYPT20121228160843692), Shenzhen High Density Electronic Packaging and Device Assembly Key Laboratory (ZDSYS20140509174237196), Shenzhen Basic Research Plan (JCYJ20140610152828685 and GJHS20120702091802836).

References

1 X. H. Huang, P. K. Jain, I. H. El-Sayed and M. A. El-Sayed, *Nanomedicine-Uk*, 2007, **2**, 681.
2 D. L. Huber, *Small*, 2005, **1**, 482.
3 R. C. Jin, *Nanoscale*, 2015, **7**, 1549.
4 R. Narayanan and M. A. El-Sayed, *Nano Lett.*, 2004, **4**, 1343.
5 Y. J. Song, H. Modrow, L. L. Henry, C. K. Saw, E. E. Doomes, V. Palshin, J. Hormes and C. S. S. R. Kumar, *Chem. Mater.*, 2006, **18**, 2817.
6 W. J. Luo, C. F. Zhu, S. Su, D. Li, Y. He, Q. Huang and C. H. Fan, *ACS Nano*, 2010, **4**, 7451.
7 C. Wang, G. J. Xiao, Y. M. Sui, X. Y. Yang, G. Liu, M. J. Jia, W. Han, B. B. Liu and B. Zou, *Nanoscale*, 2014, **6**, 15059.
8 Y. Zhang, P. L. Zhu, G. Li, T. Zhao, X. Z. Fu, R. Sun, F. Zhou and C. P. Wong, *ACS Appl. Mater. Interfaces*, 2014, **6**, 560.
9 M. Bicer and I. Sisman, *Powder Technol.*, 2010, **198**, 279.

10 D. Mott, J. Galkowski, L. Y. Wang, J. Luo and C. J. Zhong, *Langmuir*, 2007, **23**, 5740.
11 M. J. Li, K. Xiang, G. Q. Luo, D. R. Gong, Q. Shen and L. M. Zhang, *Chinese J. Chem.*, 2013, **31**, 1285.
12 P. H. Zhang, Y. M. Sui, C. Wang, Y. N. Wang, G. L. Cui, C. Z. Wang, B. B. Liu and B. Zou, *Nanoscale*, 2014, **6**, 5343.
13 A. Panacek, L. Kvitek, R. Prucek, M. Kolar, R. Vecerova, N. Pizurova, V. K. Sharma, T. Nevecna and R. Zboril, *J. Phys. Chem. B*, 2006, **110**, 16248.
14 X. L. Ren, D. Chen and F. Q. Tang, *J. Phys. Chem. B*, 2005, **109**, 15803.
15 A. J. Biacchi and R. E. Schaak, *ACS Nano*, 2015, **9**, 1707.
16 K. An and G. A. Somorjai, *Chemcatchem*, 2012, **4**, 1512.
17 V. Iablokov, S. K. Beaumont, S. Alayoglu, V. V. Pushkarev, C. Specht, J. H. Gao, A. P. Alivisatos, N. Kruse and G. A. Somorjai, *Nano Lett.*, 2012, **12**, 3091.
18 A. Panacek, R. Prucek, J. Hrbac, T. Nevecna, J. Steffkova, R. Zboril and L. Kvitek, *Chem. Mater.*, 2014, **26**, 1332.
19 A. J. Biacchi and R. E. Schaak, *ACS Nano*, 2011, **5**, 8089.
20 T. Yu, T. Koh and B. Lim, *J. Nanosci. Nanotechno.*, 2013, **13**, 3250.
21 Q. A. Zhang, W. Y. Li, C. Moran, J. Zeng, J. Y. Chen, L. P. Wen and Y. N. Xia, *J. Am. Chem. Soc.*, 2010, **132**, 11372.
22 R. Kaur, C. Giordano, M. Gradzielski and S. K. Mehta, *Chem-Asian J.*, 2014, **9**, 189.
23 J. A. Creighton and D. G. Eadon, *J. Chem. Soc., Faraday Trans.*, 1991, **87**, 3881.
24 M. A. Mahmoud, F. Saira and M. A. El-Sayed, *Nano Lett.*, 2010, **10**, 3764.
25 J. Zeng, Q. Zhang, J. Y. Chen and Y. N. Xia, *Nano Lett.*, 2010, **10**, 30.
26 Y. Zhang, P. L. Zhu, L. Chen, G. Li, F. R. Zhou, D. Q. Lu, R. Sun, F. Zhou and C. P. Wong, *J. Mater. Chem. A*, 2014, **2**, 11966.
27 Z. Y. Zhang, C. L. Shao, Y. Y. Sun, J. B. Mu, M. Y. Zhang, P. Zhang, Z. C. Guo, P. P. Liang, C. H. Wang and Y. C. Liu, *J. Mater. Chem.*, 2012, **22**, 1387.
28 N. Vilar-Vidal, J. Rivas and M. A. Lopez-Quintela, *ACS Catal.*, 2012, **2**, 1693.
29 M. H. Shao, A. Peles and K. Shoemaker, *Nano Lett.*, 2011, **11**, 3714.
30 V. K. Gupta, N. Atar, M. L. Yola, Z. Ustundag and L. Uzun, *Water Res.*, 2014, **48**, 210.
31 P. H. Zhang, Y. M. Sui, G. J. Xiao, Y. N. Wang, C. Z. Wang, B. B. Liu, G. T. Zou and B. Zou, *J. Mater. Chem. A*, 2013, **1**, 1632.
32 A. M. Kalekar, K. K. K. Sharma, A. Lehoux, F. Audonnet, H. Remita, A. Saha and G. K. Sharma, *Langmuir*, 2013, **29**, 11431.
33 H. Yamamoto, H. Yano, H. Kouchi, Y. Obora, R. Arakawa and H. Kawasaki, *Nanoscale*, 2012, **4**, 4148.
34 M. S. Usman, M. E. El Zowalaty, K. Shameli, N. Zainuddin, M. Salama and N. A. Ibrahim, *Int. J. Nanomed.*, 2013, **8**, 4467.
35 S. Mohan, O. S. Oluwafemi, S. C. George, V. P. Jayachandran, F. B. Lewu, S. P. Songca, N. Kalarikkal and S. Thomas, *Carbohyd. Polym.*, 2014, **106**, 469.
36 R. Prucek, J. Tucek, M. Kilianova, A. Panacek, L. Kvitek, J. Filip, M. Kolar, K. Tomankova and R. Zboril, *Biomaterials*, 2011, **32**, 4704.
37 B. J. Li, Y. Y. Li, Y. H. Wu and Y. B. Zhao, *Mat. Sci. Eng. C-Mater.*, 2014, **35**, 205.
38 S. Lokina, A. Stephen, V. Kaviyarasan, C. Arulvasu and V. Narayanan, *Eur. J. Med. Chem.*, 2014, **76**, 256.
39 C. P. Adams, K. A. Walker, S. O. Obare and K. M. Docherty, *Plos One*, 2014, **9**, e85981.
40 V. K. Vidhu and D. Philip, *Spectrochim. Acta A*, 2014, **117**, 102.